

## Characteristics and prevalence of *KRAS*, *BRAF*, and *PIK3CA* mutations in colorectal cancer by high-resolution melting analysis in Taiwanese population

Li-Ling Hsieh<sup>a,c</sup>, Tze-Kiong Er<sup>a,c</sup>, Chih-Chieh Chen<sup>d</sup>, Jan-Sing Hsieh<sup>e</sup>, Jan-Gowth Chang<sup>a,f</sup>, Ta-Chih Liu<sup>a,b,f,\*</sup>

<sup>a</sup> Division of Molecular Diagnostics, Department of Laboratory Medicine, Kaohsiung Medical University Hospital, Kaohsiung, Taiwan

<sup>b</sup> Division of Hematology and Oncology, Department of Internal Medicine, Kaohsiung Medical University Hospital, Kaohsiung, Taiwan

<sup>c</sup> Graduate Institute of Medicine, College of Medicine, Kaohsiung Medical University, Kaohsiung, Taiwan

<sup>d</sup> Institute of Bioinformatics and Systems Biology, National Chiao Tung University, Hsinchu, Taiwan

<sup>e</sup> Department of Surgery, Kaohsiung Medical University Hospital, Kaohsiung, Taiwan

<sup>f</sup> Institute of Clinical Medicine, College of Medicine, Kaohsiung Medical University, Kaohsiung, Taiwan

### ARTICLE INFO

#### Article history:

Received 17 April 2012

Received in revised form 27 April 2012

Accepted 28 April 2012

Available online 8 May 2012

#### Keywords:

Colorectal cancer

*KRAS* gene

*BRAF* gene

*PIK3CA* gene

Direct sequencing

High-resolution melting

### ABSTRACT

**Background:** The identification of *KRAS*, *BRAF*, and *PIK3CA* mutations before the administration of anti-epidermal growth factor receptor therapy of colorectal cancer has become important. The aim of the present study was to investigate the occurrence of *KRAS*, *BRAF*, and *PIK3CA* mutations in the Taiwanese population with colorectal cancer. This study was undertaken to identify *BRAF* and *PIK3CA* mutations in patients with colorectal cancer by high-resolution melting (HRM) analysis. HRM analysis is a new gene scan tool that quickly performs the PCR and identifies sequence alterations without requiring post-PCR treatment.

**Methods:** In the present study, DNAs were extracted from 182 cases of formalin-fixed, paraffin-embedded (FFPE) colorectal cancer samples for clinical *KRAS* mutational analysis by direct sequencing. All the samples were also tested for mutations within *BRAF* V600E and *PIK3CA* (exons 9 and 20) by HRM analysis.

**Results:** The results were confirmed by direct sequencing. The frequency of *BRAF* and *PIK3CA* mutations is 1.1% and 7.1%, respectively. Intriguingly, we found that nine patients (4.9%) with the *KRAS* mutation were coexistent with the *PIK3CA* mutation. Four patients (2.2%) without the *KRAS* mutation were existent with the *PIK3CA* mutation. Two patients (1.1%) without the *KRAS* mutation were existent with the *BRAF* mutation.

**Conclusions:** In the current study, we suppose that HRM analysis is rapid, feasible, and powerful diagnostic tool for the detection of *BRAF* and *PIK3CA* mutations in a clinical setting. Additionally, our results indicated the prevalence of *KRAS*, *BRAF*, and *PIK3CA* mutational status in the Taiwanese population.

© 2012 Elsevier B.V. All rights reserved.

### 1. Introduction

Colorectal cancer (CRC) is the third most frequent tumor worldwide, with > 70,000 new cases per year for both sexes in the United States [1]. Similarly, CRC is the third leading cause of cancer deaths in both sexes in the Taiwanese population [2]. Recently, significant improvements have been made in patient survival, after metastasis development, by improving new therapies. Anti-EGFR-targeted therapies with monoclonal antibodies such as cetuximab and panitumumab are a successful strategy for the treatment of metastatic CRC or after the failure of conventional chemotherapy. These agents bind the epidermal growth receptor (EGFR) on tumors cells and then block the downstream intracellular signaling pathways. One member of this pathway is *KRAS* and much evidence shows that the patients with *KRAS* mutations do not benefit from

the addition of cetuximab or panitumumab to standard chemotherapy [3]. Therefore, *KRAS* mutation testing should be performed in all individuals with advanced CRC refractory to first-line regimens to identify which patient's tumors will not respond to the expensive monoclonal antibody inhibitors of EGFR.

*KRAS* encodes a membrane-associated GTPase that is an early player in many signal transduction pathways. *KRAS* acts as a molecular on/off switch that recruits and activates proteins that are necessary for the propagation of growth factor and other receptor signals, such as c-Raf and PI 3-kinase. When activated, *KRAS* is involved in the dephosphorylation of GTP to GDP, after which it is turned off. The rate of GTP to GDP conversion can be dramatically accelerated by an accessory protein of the guanine nucleotide activating protein (GAP) class, for example, RasGAP [4]. In CRCs, *KRAS* point mutations occur early in the adenoma-carcinoma sequence and are believed to contribute to the growth and increased atypia of adenomas [5]. Activating mutations of the *KRAS* gene have been widely studied as markers for cancer prognosis. These gene mutations, principally in codons 12 and 13, occur in approximately one-half of CRCs, and population-based studies have suggested that the mutations might be associated with some tumor phenotypes [6]. Recently,

\* Corresponding author at: Division of Molecular Diagnostic, Department of Laboratory Medicine, Kaohsiung Medical University Hospital, 100 Shih-Chuan 1st Rd., Kaohsiung, Taiwan.

E-mail address: [d730093@cc.kmu.edu.tw](mailto:d730093@cc.kmu.edu.tw) (T.-C. Liu).

high-resolution melting (HRM) analysis has been applied for use in the screening for the *KRAS* mutation in CRC [7].

*BRAF*, a member of the *RAF* gene family (*BRAF*, *ARAF1*, and *RAF1*), encodes a serine–threonine protein kinase that is a downstream effector of activated *KRAS*. Mutated *BRAF* activates a signaling cascade involving proteins in the mitogen-activated protein kinase system, resulting in cell proliferation [8]. Approximately 15% of CRC have the *BRAF* mutation and this is relevant to poor prognosis [9]. The hotspot mutation is the T-to-A transversion at nucleotide 1796 causing V600E. This mutation is predisposed to the inhibition of apoptosis and also aids in increasing invasiveness [10]. Meanwhile, *KRAS* and *BRAF* mutations are mutually exclusive in CRC [11]. This suggests that they occur in different tumor types and might have different outcomes. On the other hand, studies showed that the *BRAF* V600E mutation confers resistance to EGFR monoclonal antibodies in patients with chemotherapy-refractory *KRAS*-wild-type metastatic CRC [12]. Moreover, a part of CRC patients without in *KRAS* and *BRAF* mutations fails to respond to anti-EGFR therapy, and this may be due to mutations in the *PIK3* gene.

The *PIK3*s are a family of lipid kinases that are grouped into classes with a different structure and substrate preference [13]. *PIK3*Ks are heterodimeric kinases that are involved in the control of cellular growth, transformation, adhesion, and also apoptosis [14]. Several studies showed that the p110 $\alpha$  isoform which is encoded by *PIK3CA* is mutated in approximately 15–18% of CRCs [15,16]. In CRCs, more than 80% of *PIK3CA* mutations occur in either exon 9 or exon 20 [11].

HRM analysis is rapidly becoming the most important mutation-scanning methodology that allows mutation scanning and genotyping without the need for costly labeled oligonucleotides. It is a closed-tube method, indicating that PCR amplification and subsequent analysis are sequentially performed in the well, making it more convenient than other scanning methodologies. Recently, we have used this method of genotyping and mutation scanning [7,17,18]. The aim of this study was to understand the *KRAS*, *BRAF*, and *PIK3CA* gene status in a Taiwanese cohort of CRC patients using direct DNA sequencing and HRM analysis.

## 2. Materials and methods

### 2.1. Sample preparation and DNA extraction

The specimens consisted of 182 formalin-fixed, paraffin-embedded (FFPE) colorectal adenocarcinomas submitted for clinical *KRAS* mutational analysis. All samples were tested for *BRAF* V600E and *PIK3CA* mutations within exon 9 and exon 20. FFPE samples were deparaffinized and air dried, subsequently, DNA was isolated using the proteinase K and QIAamp $\text{®}$  micro DNA extraction kit (QIAGEN) according to the manufacturer's protocol.

### 2.2. Design of primers for HRM assay

A good amplicon design is essential for obtaining robust and reproducible HRM analysis. The difference between wild-type and heterozygote curves becomes smaller and more difficult to differentiate when the product length increases. Besides, extra care is needed to design PCR reactions that avoid primer dimers and non-specific amplification in HRM analysis.

DNA samples were amplified for the *KRAS* regions, including codons 12 and 13, using primers according to the previously published works [7]. The 153 bp PCR products with a single band were resolved on 2% agarose gels and visualized after staining with ethidium bromide. The cycling conditions for *KRAS* codons 12 and 13 involved a 35-cycle PCR program (denaturation at 96 °C for 10 s; annealing at 50 °C for 5 s; and elongation at 60 °C for 4 min). Mutation status was determined by direct sequencing.

The set of primers for HRM, specific for *BRAF* V600E and *PIK3CA* exon 9 and exon 20, were designed while fulfilling the requirements of the LightCycler $\text{®}$  480 System Gene Scanning Assay. All the amplicons were

designed to be smaller than 300 bp. In the present study, the three pairs of primers for HRM analysis were selected using Primer3 software (Table 1). Appropriate primers were named as H1–H6 as shown in Table 1. All the primers synthesized were all of standard molecular biology quality (Protech Technology Enterprise Co., Ltd, Taiwan).

### 2.3. The HRM technique

PCR reactions were carried out in a 10  $\mu$ l final volume using the LightCycler $\text{®}$  480 High-Resolution Melting Master (Reference 04909631001, Roche Diagnostics) 1 $\times$  buffer – containing Taq polymerase, nucleotides and the dye ResoLight – and 20 ng DNA. The primers and MgCl $_2$  were used at a concentration of 0.25  $\mu$ M and 2.5 mM, respectively, for identifying the mutation status of *BRAF* V600E, *PIK3CA* exon 9, and exon 20.

The HRM assays were conducted using the LightCycler $\text{®}$  480 Instrument (Roche Diagnostics) provided with the software LightCycler $\text{®}$  480 Gene Scanning Software Version 1.5 (Roche Diagnostics).

The PCR program required a SYBR Green I filter (533 nm), and it consisted of an initial denaturation–activation step at 95 °C for 10 min, followed by a 45-cycle program (denaturation at 95 °C for 15 s, annealing at 60 °C or 62 °C (Table 1) for 15 s, and elongation at 72 °C for 15 s with reading of the fluorescence; acquisition mode: single). The melting program included three steps: denaturation at 95 °C for 1 min, renaturation at 40 °C for 1 min, and subsequent melting that consists of a continuous fluorescent reading of fluorescence from 60 to 90 °C at the rate of 25 acquisitions per °C.

### 2.4. Gene scanning

The melting curve analysis performed by the Gene Scanning Software consists of three steps: normalization of melting curves, which involves equaling to 100% of the initial fluorescence and to 0% of the fluorescence remnant after DNA dissociation: shifting of the temperature axis of the normalized melting curves to the point where the entire double-stranded DNA is completely denatured: and, finally, the generation of difference plots, allowing the capture of the differences in melting profile between the reference sample curves from the test samples. If the shape of the melting curves is not similar to each other, then we will confirm it by direct DNA sequencing to prevent a false negative result. Furthermore, an analysis of the melting curves with a high-sensitivity setting of 0.5 was carried out by Gene Scanning Software (the default sensitivity setting of the Gene Scanning Software is 0.3.).

### 2.5. Direct sequencing

To confirm the results of HRM analysis, sequencing analysis was also performed in all samples. After HRM analysis, the samples were purified using a PCR-M $\text{™}$  clean-up system (VIOGEN, Sunnyvale CA 94086, U.S.A.). The PCR products generated after HRM were directly sequenced. The sequence reaction was performed in a final volume of 10  $\mu$ l, including 1  $\mu$ l of the purified PCR product, 2.5  $\mu$ M of one of the PCR primers, 2  $\mu$ l of the ABI PRISM terminator cycle sequencing kit v3.1 (Applied Biosystems)

**Table 1**  
Primers use for HRM analysis of *BRAF* and *PIK3CA* gene mutation.

Detection for	Sequence (5' to 3')	Annealing temp. (°C)
<i>PIK3CA</i> Exon 9	H1 5'-GCCTGCTGAAAATGACTGAA-3' (forward)	58
	H2 5'-CATTITAGCACTTACCTGTGACTCCA-3' (reverse)	
<i>PIK3CA</i> Exon 20	H3 5'-TGAGCAAGAGGCTTTGGAGT-3' (forward)	58
	H4 5'-TCATTTTCTCAGTTATCTTTTCAGTTCAAT-3' (reverse)	
<i>BRAF</i>	H5 5'-CATAATGCTTCTGCTGATAGGAAA-3' (forward)	58
	H6 5'-TCAGCACATCTCAGGGCCAAA-3' (reverse)	

**Table 2**

Mutational status of 15 patients detected by HRM analysis and confirmed by direct DNA sequencing for the *BRAF* and *PIK3CA* genes.

Patient ID	<sup>a</sup> <i>KRAS</i>	<i>PIK3CA</i> (exon9)	<i>PIK3CA</i> (exon 20)	<i>BRAF</i> V600E
P1	MT	c.1633G>A	WT	WT
P2	MT	c.1633G>A	WT	WT
P3	MT	c.1633G>A	WT	WT
P4	MT	c.1634A>G	WT	WT
P5	MT	c.1634A>G	WT	WT
P6	MT	c.1634A>G	WT	WT
P7	MT	c.1633G>C	WT	WT
P8	WT	c.1634A>G	WT	WT
P9	WT	c.1633G>A	WT	WT
P10	WT	c.1633G>A	WT	WT
P11	WT	c.1634A>G	WT	WT
P12	MT	WT	c.3140A>G	WT
P13	MT	WT	c.3140A>T	WT
P14	WT	WT	WT	c.1799T>A
P15	WT	WT	WT	c.1799T>A

<sup>a</sup> *KRAS* mutation was identified by direct sequencing WT: wild-type MT: mutant.

and 2  $\mu$ l 5 $\times$  sequence buffer. The sequencing program is a 25-cycle PCR program (denaturation at 96 °C for 10 s; annealing at 50 °C for 5 s; and elongation at 60 °C for 4 min). The sequence detection was performed in the ABI Prism 3130 Genetic Analyzer (Applied Biosystems) according to standard protocols.

### 3. Results

#### 3.1. Mutational status

*KRAS* mutations were detected in 61 patients (33.5%) by direct sequencing. In particular, only 2 (P14 and P15) patients harbor *BRAF* mutations, and all these were *KRAS* wild-type tumors, as shown in Table 2. None of the 61 CRC patients with *KRAS* mutations harbors a concomitant mutation in *BRAF*. Intriguingly, concomitant *PIK3CA* and *KRAS* mutations were observed in 9 patients (P1~P7, P12, and P13), as shown in Table 2. On the other hand, 4 patients (P8~P11) harbor *PIK3CA* mutations, and all these were *KRAS* wild-type tumors, as shown in Table 2. The frequency of *KRAS*, *BRAF*, and *PIK3CA* mutational status is summarized in Fig. 4.

#### 3.2. Application of HRM analysis for the *PIK3CA* mutation analysis in colorectal samples by HRM analysis

The normalized and temperature-shifted difference plots, the melting profile obtained from CRCs carrying mutation of the *PIK3CA* mutation in exon 9 were shown in Fig. 1(A). Each mutation (c.1634G>C, c.1633G>A, and c.1633A>G) could be readily and accurately identified in the difference plot curves. Sequencing analysis was performed in all samples using the same PCR products after melting analysis. As previously described, the results of the HRM analysis were confirmed by

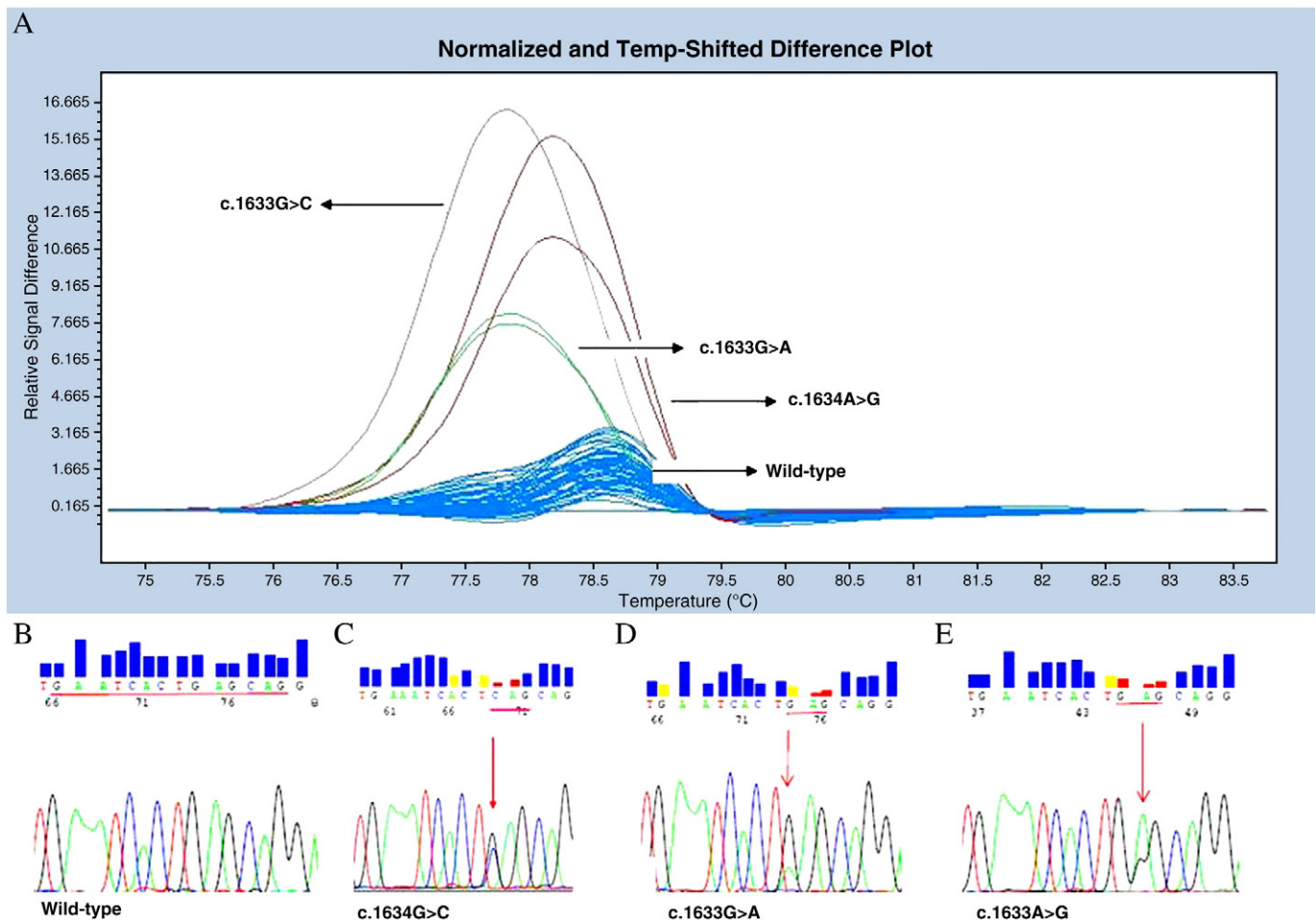


**Fig. 1.** Representative cases of *PIK3CA* gene (exon 9) detection in patients with CRC using HRM analysis. (A) The normalized and temperature-shifted difference plot for the mutation screening of *PIK3CA* gene (exon 9). Sequencing results confirm the (B) wild-type and the presence of the *PIK3CA* gene (exon 9) mutation: (C) c.1634G>C, (D) c.1633G>A, (E) c.1633A>G.

direct sequencing. The electropherograms of representative patients with WT samples and the *PIK3CA* mutation in exon 9 were shown in Fig. 1(B)–(D).

In addition, the normalized and temperature-shifted difference plots, the melting profile obtained from CRCs carrying the *PIK3CA* mutation in exon 20 were shown in Fig. 2(A). Each mutation (c.3140A>G and c.3140A>T) could be readily and accurately identified in the difference plot curves. The electropherograms of the representative patients with WT samples and the *PIK3CA* mutation in exon 20 were shown in Fig. 1(B)–(C).

### 3.3. Application of HRM analysis for the *BRAF* V600E mutation analysis in colorectal samples by HRM analysis

The normalized and temperature-shifted difference plots, the melting profile obtained from CRCs carrying mutation of the *BRAF* V600E mutation were shown in Fig. 3(A). The mutation (c.1799T>A) could be readily and accurately identified in the difference plot curves. Sequencing analysis was performed in all samples using the same PCR products after melting analysis. As previously described, the results of HRM analysis were confirmed by direct sequencing. The electropherograms of the representative patients with WT samples and the *BRAF* V600E mutation were shown in Fig. 3(B)–(C).

## 4. Discussion

Nowadays, mutation analysis of definite genes has already been incorporated in the treatment of CRC patients. Therefore, the demand for a fast and reliable diagnostic tool is increasing. The aim of this study was to develop a sensitive test that allows the molecular characterization of hotspot mutations in *BRAF* and *PIK3CA* genes. In this study, we have successfully established a diagnostic strategy by HRM analysis for identifying the *BRAF* and *PIK3CA* mutations of 182 CRC patients in southern Taiwan. On the other hand, we demonstrate the distribution of *KRAS*, *BRAF* and *PIK3CA* gene mutations in a Taiwanese population.

HRM is rapidly gaining acceptance as the most important mutation scanning methodology. It is a closed-tube method, indicating that PCR amplification and subsequently analysis are sequentially performed in the well. This makes it more convenient than other scanning methodologies. The differences between the WT and heterozygote curves become smaller and more difficult to differentiate when the product length increases [19]. In fact, all of the heterozygous mutants are easily identified from their melting curves. Heterozygotes were easily identified because heteroduplexes altered the shape of the melting curves [19]. These differences are best visualized using difference plots because slight differences in curve shape and melting temperature ( $T_m$ ) become obvious. Moreover, direct sequencing was still the gold-standard methodology in most clinical laboratories to detect and confirm gene mutation. However, direct

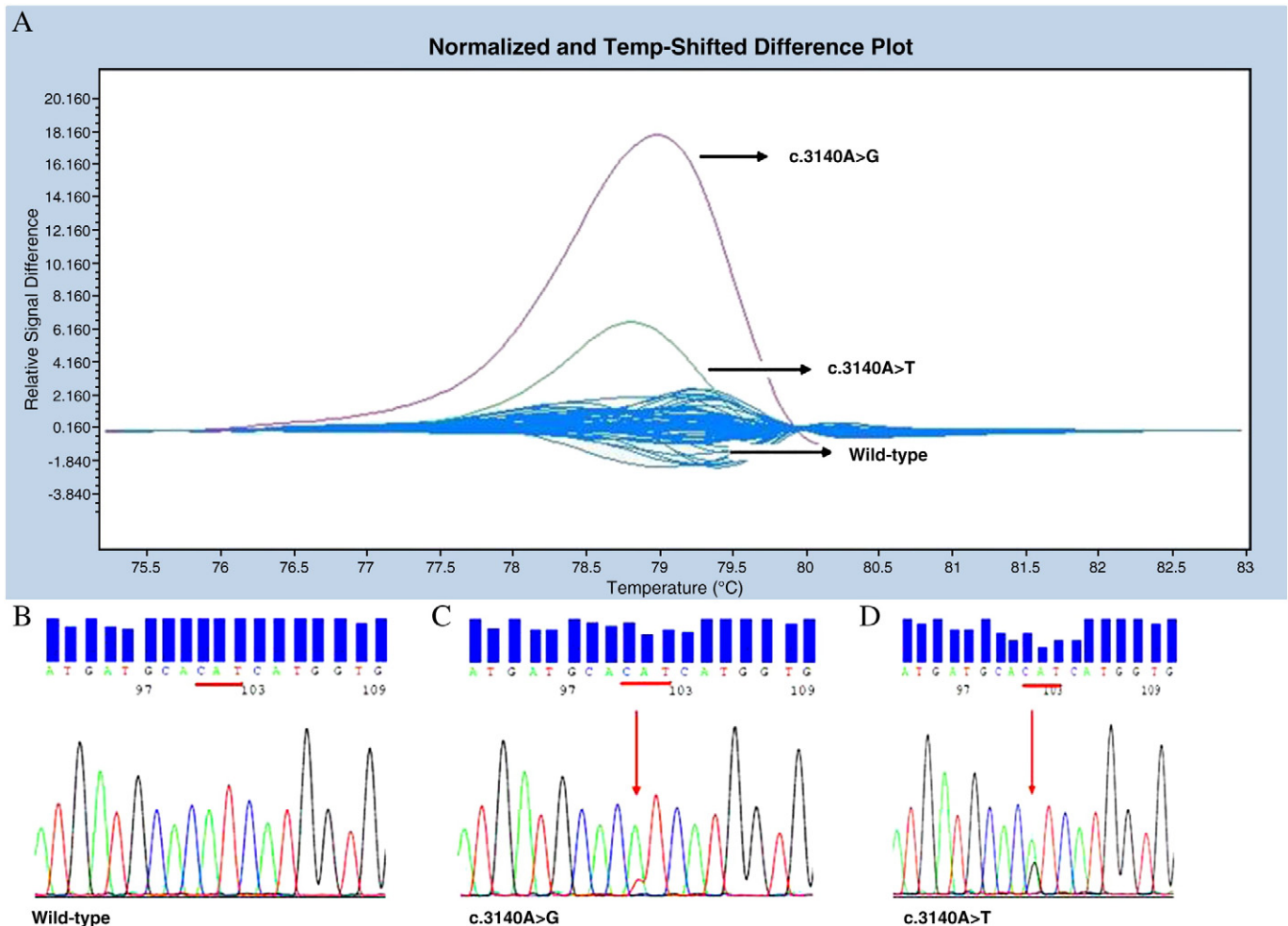
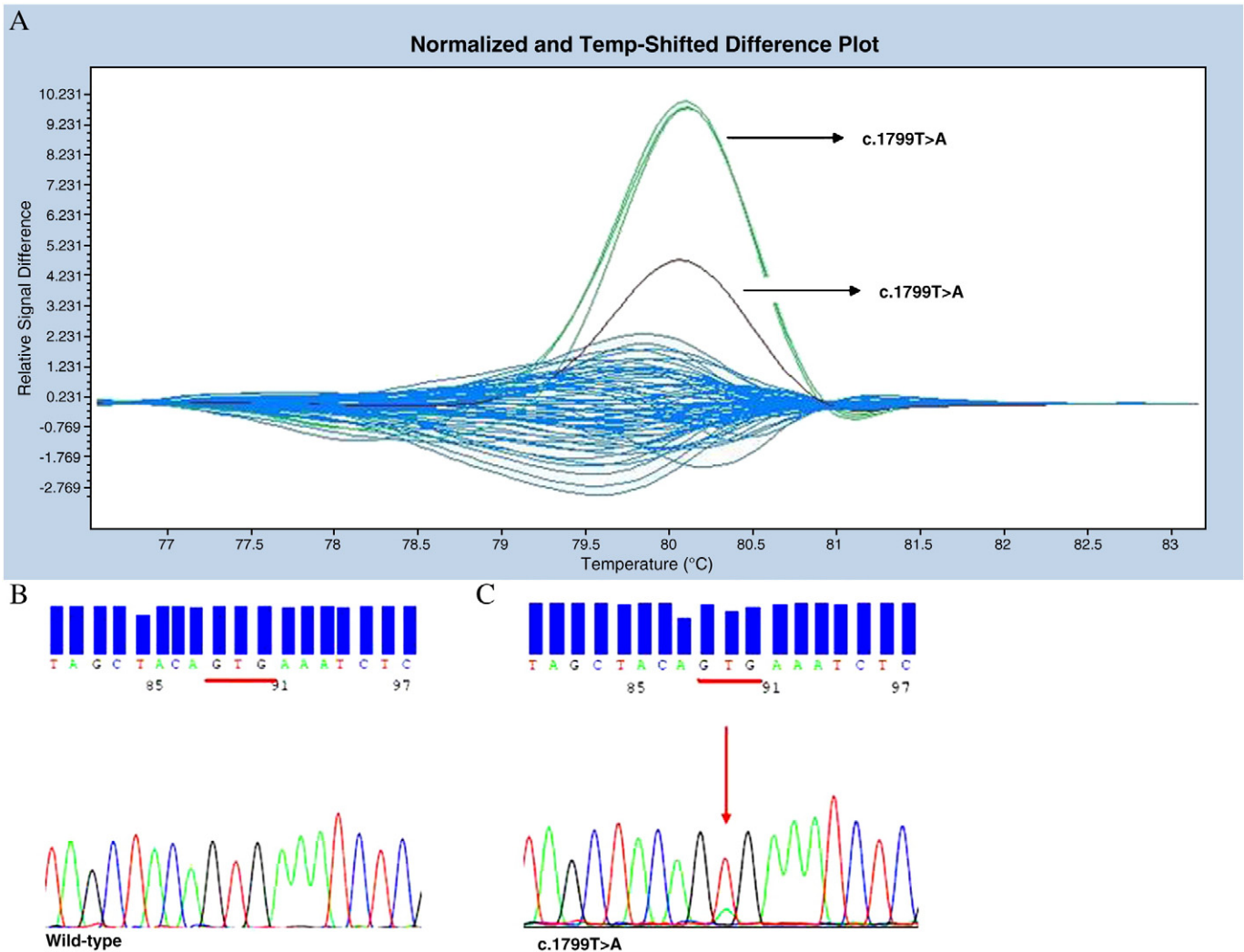


Fig. 2. Representative cases of *PIK3CA* gene (exon 20) detection in patients with CRC using HRM analysis. (A) The normalized and temperature-shifted difference plot for the mutation screening of *PIK3CA* gene (exon 20). Sequencing results confirm the (B) wild-type and the presence of the *PIK3CA* gene (exon 20) mutation: (C) c.3140A>G, (D) c.3140A>T.





**Fig. 3.** Representative cases of *BRAF* gene (V600E) detection in patients with CRC using HRM analysis. (A) The normalized and temperature-shifted difference plot for the mutation screening of *BRAF* gene (V600E). Sequencing results confirm the (B) wild-type and the presence of the *BRAF* gene mutation: (C) c.1799T>A.

sequencing is rarely sensitive below 10% mutant allele frequency, which corresponds to a threshold of 25% tumor cells that are heterozygous for a mutation [20,21]. Earlier, we had demonstrated that the analytical sensitivity was 5% for screening of the *KRAS* mutation using HRM analysis [7]. Our previous report indicated that HRM analysis is a double-edged sword having both advantages and disadvantages. The disadvantage of the HRM analysis is its inability to identify which codon is mutated. The advantage of HRM analysis however, is its feasibility and high accuracy method for screening gene mutation. In addition, the PCR amplification products obtained from HRM analysis could be directly used for direct sequencing without any pretreatment. If the clinical sample is detected by HRM as the wild-type form, then all the wild-type results can be quickly reported to the clinicians. Thus, employing HRM analysis for the wild types can be quickly ruled out in large-scale clinical samples. In the current study, if an abnormal melting curve is noted, then the precise mutation should be confirmed by direct sequencing.

*KRAS* and *BRAF* mutations that are mutually exclusive in CRCs have been previously reported in several studies [22,23]. Similarly, the analysis of our results confirmed that none of the 182 CRCs with *KRAS* mutations had a concomitant mutation in *BRAF*. Numerous studies have implicated the frequency of *BRAF* mutations in different populations. The overall *BRAF* V600E mutational rate ranges from 3.3% to 13% in the different populations. Two recent studies demonstrated that the frequency of *BRAF* mutations is approximately 6.25% and 13% in CRCs patients, respectively, in the Spanish population [24,25]. Similarly, Nicolantonio

et al. [23] found that the *BRAF* mutation is approximately 10% of CRCs. Simi L and et al. [26] demonstrated that the frequency of *BRAF* mutations is approximately 9.5% of CRCs patients in the Italian population. Saridaki et al. [27] indicated that the frequency of *BRAF* mutations is 7.2% of CRCs in the Greece population. In the Asian population, Li HT et al. showed that the frequency of the *BRAF* mutations is approximately 7% of CRCs in the Chinese population [28], and Kwon MJ et al. showed that the frequency of the *BRAF* mutations is approximately 3.3% of CRCs in the Korean population [29]. In the Taiwanese population, the frequency of *BRAF* mutations is reported as being about 3.8% of 314 CRCs patients [30]. It should be noted that the frequency of *BRAF* mutations is 1.1% of the *KRAS* wild-type patients (as shown in Fig. 5) in the present study. We suppose that the lower frequency of *BRAF* mutations in our series of CRC patients could be due to the small sample size and different ethnic populations. Future works are required to confirm these data by including more CRC samples.

As just mentioned, the *PIK3CA* mutation has also been suggested as being a biomarker of anti-EGFR monoclonal antibody resistance. Till very recently, the correlation between *PIK3CA* mutations and the response to the anti-EGFR monoclonal antibody is still a debating issue [31,32]. There are numerous discrepancies in the *PIK3CA* gene mutational status reported from several studies, and the results indicated different percentages ranging from 6.5% to 18% [11,15,16]. Most of the studies showed the distribution of *PIK3CA* hotspot mutations located at exon 9 and exon 20, whereas mutations that appear at exon 9 were the

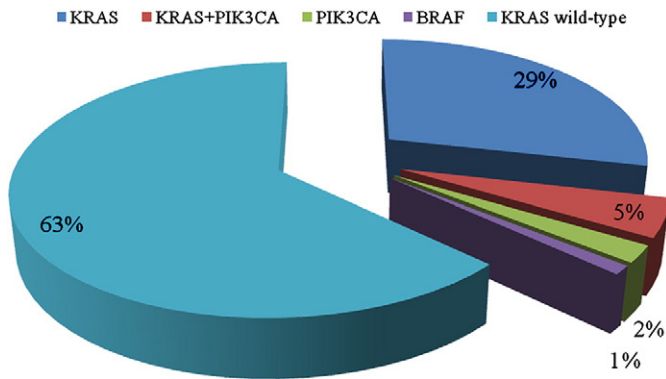


Fig. 4. Frequency of *KRAS*, *BRAF*, and *PIK3CA* mutational status.

most frequent [15,16]. The *PIK3CA* mutations were detected in approximately 13% of CRC patients in the United States and European countries [11,16,31–33]. In the Chinese and Korean population, the frequency of the *PIK3CA* mutations that were detected in CRC patients is 12.5% and 6.5%, respectively [28,29]. In the present study, we showed that 7.1% of CRC patients harbor *PIK3CA* mutations, and our results were similar to those by Kwon MJ et al. [29], who indicated that the prevalence of *PIK3CA* mutations in 92 CRC patients was 6.5% using the PNA-mediated PCR clamping method. Intriguingly, Lin JK et al. [34] showed that no *PIK3CA* mutation was found in 42 metastatic CRC patients in the Taiwanese population. It should also be noted that about 30% of *PIK3CA* somatic mutations couple with another oncogene mutation, especially represented by the *KRAS* gene [35]. Besides, the presence of *PIK3CA* mutations was associated with a poor prognosis and with an increase in colorectal cancer-specific mortality [36]. Our results showed that 9 patients (4.9%) with the *KRAS* mutation were coexistent with the *PIK3CA* mutation and 4 patients (2.2%) without the *KRAS* mutation were coexistent with the *PIK3CA* mutation (as shown in Fig. 4). In the present study, we did not provide relevant information about patients' responses, therefore, future works are required to prove whether some patients who present *PIK3CA* could be responders to anti-EGFR therapies or not.

In the current study, we also intended to model the proteins encoded by *BRAF* and *PIK3CA* genes, respectively, in order to understand the structural implications of the mutations identified in this study. The atomic

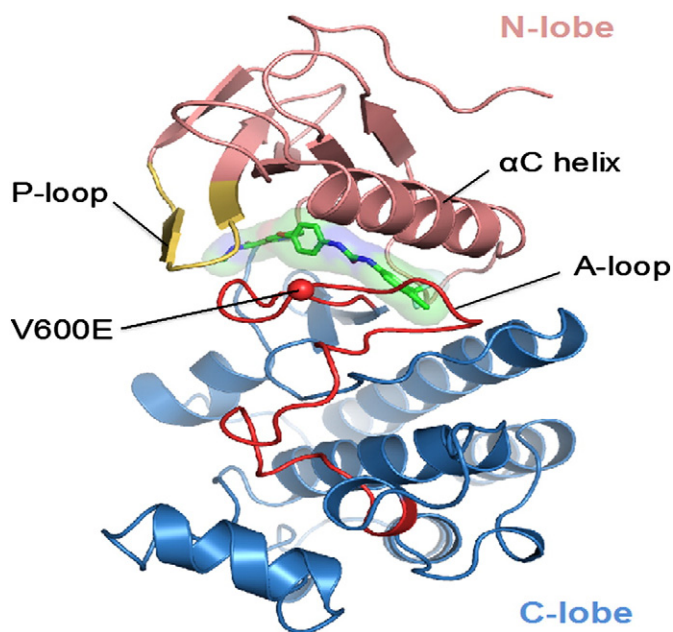


Fig. 5. The structure of human *BRAF* protein.

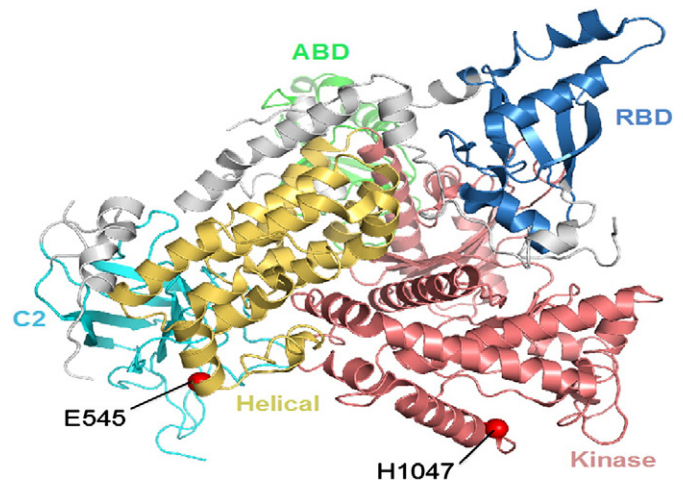


Fig. 6. The structure of human p110 $\alpha$  protein.

coordinates of the crystal structure for the human *BRAF* kinase domain were retrieved from the protein data bank [37] (PDB entry: 1UWH [38]). The region not solved in the crystal structure, residues 601–612, was modeled using the loop-building routine in MODELLER [39]. The model of human *BRAF* model is shown in Fig. 5. Most of the mutations of *BRAF* are clustered in two different regions within the binding pocket: (1) the glycine-rich P-loop (yellow) of the N-lobe; (2) the activation segment, A-loop (red). The *BRAF* hotspot mutation, V600E, located at the A-loop is highlighted in red spheres. This mutation may disrupt an inactive conformation of *BRAF* kinase [38]. Therefore, *BRAF* V600E increases the kinase activity that provides cancer cells with both proliferation and survival signals and promotes them to become tumors in the model system [38].

The crystal structure of Human p110 $\alpha$  (p110 $\alpha$ ; encoded by the *PIK3CA* gene) was obtained from the protein data bank [37] (PDB entry: 2RD0 [40] (Fig. 6)). Most of the reported mutations are reported in the *PIK3CA* cluster in conserved regions within the region coding for the helical (yellow) and kinase (red) domain of p110 $\alpha$  [41]. Indeed, the *PIK3CA* mutations identified in the current study, the E545 and H1047, are located at the helical domain and kinase domain, respectively. The residues of E545 and H1047 are highlighted in red spheres (Fig. 6). Studies showed that mutant E545 inhibits the activity of the catalytic subunit, because it interacts with L379 and A340 of the p85 nSH2 domain [42]. The mutant H1047 has a direct effect on the conformation of the activation loop, changing its interaction with phosphatidylinositol substrates [40].

In conclusion, we demonstrate that HRM analysis is a rapid, feasible, and powerful diagnostic tool for the detection of *BRAF* and *PIK3CA* mutations in a clinical setting. Additionally, our results indicated the prevalence of *KRAS*, *BRAF*, and *PIK3CA* mutational status in the Taiwanese population.

#### Acknowledgments

We are grateful to both the hardware and software supports of the Structural Bioinformatics Core Facility at National Chiao Tung University.

#### References

- [1] Jemal A, Bray, Center MM, et al. Global cancer statistics. *CA Cancer J Clin* 2011;61: 69–90.
- [2] Department of Health. Health and vital statistics. Taipei: Department of Health, Executive Yuan; 2007.
- [3] Allegra CJ, Jessup JM, Somerfield MR, et al. American Society of Clinical Oncology provisional clinical opinion: testing for *KRAS* gene mutations in patients with metastatic colorectal carcinoma to predict response to anti-epidermal growth factor receptor monoclonal antibody therapy. *J Clin Oncol* 2009;27:2091–6.
- [4] Chang DZ, Kumar V, Ma Y, et al. Individualized therapies in colorectal cancer: *KRAS* as a marker for response to EGFR-targeted therapy. *J Hematol Oncol* 2009;22:2–18.

- [5] Fearon ER, Vogelstein B. A genetic model for colorectal tumorigenesis. *Cell* 1990;61:759–67.
- [6] Park JH, Kim IJ, Kang HC, et al. Oligonucleotide microarray-based mutation detection of the K-ras gene in colorectal cancers with use of competitive DNA hybridization. *Clin Chem* 2004;50:1688–91.
- [7] Er TK, Chang YS, Yeh KT, et al. Comparison of two different methods for the screening of *KRAS* mutation in colorectal cancer. *Clin Lab* 2010;56:175–86.
- [8] Kolch W. Meaningful relationships: the regulation of the Ras/Raf/MEK/ERK pathway by protein interactions. *Biochem J* 2000;351:289–305.
- [9] Roth AD, Tejpar S, Delorenzi M, et al. Prognostic role of *KRAS* and *BRAF* in stage II and III resected colon cancer: result of the translational study on the PETACC-3, EORTC 40933, SAKK 60-00 trial. *J Clin Oncol* 2010;28:466–74.
- [10] Minoo P, Moyer MP, Jass JR. Role of *BRAF*-V600E in the serrated pathway of colorectal tumorigenesis. *J Pathol* 2007;212:124–33.
- [11] De Roock W, Claes B, Bernasconi D, et al. Effects of *KRAS*, *BRAF*, *NRAS*, and *PIK3CA* mutations on the efficacy of cetuximab plus chemotherapy in the chemotherapy-refractory metastatic colorectal cancer: a retrospective consortium analysis. *Lancet Oncol* 2010;11:753–62.
- [12] Laurent-Puig P, Cayre A, Manceau G, et al. Analysis of *PTEN*, *BRAF*, and *EGFR* status in determining benefit from cetuximab therapy with wild-type *KRAS* metastatic colon cancer. *J Clin Oncol* 2009;27:5924–30.
- [13] Markman B, Atzori F, Perez-Garcia H, et al. Status of PI3K inhibition and biomarker development in cancer therapeutics. *Ann Oncol* 2010;21:683–91.
- [14] Karakas B, Bachman KE, Park BH. Mutation of the *PIK3CA* oncogene in human cancers. *Br J Cancer* 2006;94:455–9.
- Samuels Y, Ericson K. Oncogenic PI3K and its role in cancer. *Curr Opin Oncol* 2006;18:77–82.
- [15] Nosho K, Kawasaki T, Ohnishi, et al. *PIK3CA* mutation in colorectal cancer: relationship with genomic and epigenetic alterations. *Neoplasia* 2008;10:534–41.
- [16] Barault L, Veyrie N, Jooste V, et al. Mutations in the RAS-MAPK, PI(3)K (phosphatidylinositol-3-OH-kinase) signaling network correlate with poor survival in a population-based series of colon cancers. *Int J Cancer* 2008;122:2255–9.
- [17] Chang CC, Lin PC, Lin CH, et al. Rapid identification of CYP2C8 polymorphism by high resolution melting analysis. *Clin Chim Acta* 2012;413:298–302.
- [18] Lin YC, Lin YC, Liu TC, et al. High-resolution melting curve (HRM) analysis to establish CYP21A2 mutations converted from the CYP21A1P in congenital adrenal hyperplasia. *Clin Chim Acta* 2011;412:1918–23.
- [19] Reed GH, Wittwer CT. Sensitivity and specificity of single-nucleotide polymorphism scanning by high-resolution melting analysis. *Clin Chem* 2004;50:1748–54.
- [20] Pao W, Wang TY, Riely GJ, et al. *KRAS* mutations and primary resistance of lung adenocarcinomas to gefitinib or erlotinib. *PLoS Med* 2005;2:57–61.
- [21] Faller MB, Legrain M, Voegeli AC, et al. Detection of K-Ras mutations in tumor samples of patients with non-small cell lung cancer using PNA-mediated PCR clamping. *Br J Cancer* 2009;100:985–92.
- [22] Amado RG, Wolf M, Peeters M, et al. Wild-type *KRAS* is required for panitumumab efficacy in patients with metastatic colorectal cancer. *J Clin Oncol* 2008;26:1626–34 [Di].
- [23] Di Nicolantonio F, Martini M, Molinari F, et al. Wild-type *BRAF* is required for response to panitumumab or cetuximab in metastatic colorectal cancer. *J Clin Oncol* 2008;26:5705–12.
- [24] Borràs E, Jurado I, Hernan I, et al. Clinical pharmacogenomic testing of *KRAS*, *BRAF* and *EGFR* mutations by high resolution melting analysis and ultra-deep pyrosequencing. *BMC Cancer* 2011;11:406.
- [25] Herreros-Villanueva M, Rodrigo M, Claver M, et al. *KRAS*, *BRAF*, *EGFR* and *HER2* gene status in a Spanish population of colorectal cancer. *Mol Biol Rep* 2011;38:1315–20.
- [26] Simi L, Pratesi N, Vignoli M, et al. High-resolution melting analysis for rapid detection of *KRAS*, *BRAF*, and *PIK3CA* gene mutations in colorectal cancer. *Am J Clin Pathol* 2008;130:247–53.
- [27] Saridaki Z, Tzardi M, Papadaki C, et al. Impact of *KRAS*, *BRAF*, *PIK3CA* mutations, *PTEN*, *AREG*, *EREG* expression and skin rash in ≥2nd line cetuximab-based therapy of colorectal cancer patients. *PLoS One* 2011;26:e15980.
- [28] Li HT, Lu YY, An YX, et al. *KRAS*, *BRAF* and *PIK3CA* mutations in human colorectal cancer: relationship with metastatic colorectal cancer. *Oncol Rep* 2011;25:1691–7.
- [29] Kwon MJ, Lee SE, Kang SY, et al. Frequency of *KRAS*, *BRAF*, and *PIK3CA* mutations in advanced colorectal cancers: comparison of peptide nuclei acid-mediated PCR clamping and direct sequencing in formalin-fixed, paraffin-embedded tissue. *Pathol Res Pract* 2011;207:762–8.
- [30] Liou JM, Wu MS, Shun CT, et al. Mutations in *BRAF* correlate with poor survival of colorectal cancers in Chinese population. *Int J Colorectal Dis* 2011;26:1387–95.
- [31] Sartore-Bianchi A, Martini M, Molinari F, et al. *PIK3CA* mutations in colorectal cancer are associated with clinical resistance to EGFR-targeted monoclonal antibodies. *Cancer Res* 2009;69:1851–7.
- [32] Prenen H, De SJ, Jacobs B, De RW, et al. *PIK3CA* mutations are not major determination of resistance to the epidermal growth factor receptor inhibitor cetuximab in metastatic colorectal cancer. *Clin Cancer Res* 2009;15:3184–8.
- [33] Ogino S, Nosho K, Kirkner CJ, et al. *PIK3CA* mutation is associated with poor prognosis among patients with curatively resected colon cancer. *J Clin Oncol* 2009;27:1477–84.
- [34] Lin JK, Lin AJ, Lin CC, et al. The status of EGFR-associated genes could predict the outcome and tumor response of chemo-refractory metastatic colorectal patients using cetuximab and chemotherapy. *J Surg Oncol* 2011;104:661–6.
- [35] Thomas RK, Baker AC, Debiasi RM, et al. Oncogenic insertional mutations in the P-loop of Ras are overactive in MAP kinase signaling. *Oncogene* 2000;19:5367–76.
- [36] Baldus SE, Schaefer KL, Engers R, et al. Prevalence and heterogeneity of *KRAS*, *BRAF*, and *PIK3CA* mutations in primary colorectal adenocarcinomas and their corresponding metastases. *Clin Cancer Res* 2010;16:790–9.
- [37] Berman HM, Westbrook J, Feng Z, et al. The Protein Data Bank. *Nucleic Acids Res* 2000;28:235–42.
- [38] Wan PT, Garnett MJ, Roe SM, et al. Mechanisms of activation of the RAF-ERK signaling pathway by oncogenic mutation of B-RAF. *Cell* 2004;116:855–67.
- [39] Sali A, Blundell TL. Comparative protein modeling by satisfaction of spatial restraints. *J Mol Biol* 1993;234:779–815.
- [40] Huang CH, Mandelker D, Schmidt-Kittler O, et al. The structure of a human p110α/p85α complex elucidates the effects of oncogenic PI3Kα mutations. *Science* 2007;318:1744–8.
- [41] Samuels Y, Wang Z, Bardelli A, et al. High frequency of mutations of the *PIK3CA* gene in human cancers. *Science* 2004;304:554.
- [42] Miled N, Yan Y, Hon WC, et al. Mechanism of two classes of cancer mutations in the phosphoinositide 3-kinase catalytic subunit. *Science* 2007;317:239–42.